Published in final edited form as:
Cancer Res. 2007 November 1; 67(21): 10501–10510. doi:10.1158/0008-5472.CAN-07-1778.

Photodynamic Therapy Enhancement of Antitumor Immunity Is Regulated by Neutrophils

Philaretos C. Kousis, **Barbara W. Henderson**, **Patricia G. Maier**, and **Sandra O. Gollnick**
Department of Cell Stress Biology and the Photodynamic Therapy Center, Roswell Park Cancer Institute, Buffalo, New York

Abstract

Photodynamic therapy (PDT) is a Food and Drug Administration–approved local cancer treatment that can be curative of early disease and palliative in advanced disease. PDT of murine tumors results in regimen-dependent induction of an acute local inflammatory reaction, characterized in part by rapid neutrophil infiltration into the treated tumor bed. In this study, we show that a PDT regimen that induced a high level of neutrophilic infiltrate generated tumor-specific primary and memory $CD8^+$ T-cell responses. In contrast, immune cells isolated from mice treated with a PDT regimen that induced little or no neutrophilic infiltrate exhibited minimal antitumor immunity. Mice defective in neutrophil homing to peripheral tissues ($CXCR2^{-/-}$ mice) or mice depleted of neutrophils were unable to mount strong antitumor $CD8^+$ T-cell responses following PDT. Neutrophils seemed to be directly affecting T-cell proliferation and/or survival rather than dendritic cell maturation or T-cell migration. These novel findings indicate that by augmenting T-cell proliferation and/or survival, tumor-infiltrating neutrophils play an essential role in establishment of antitumor immunity following PDT. Furthermore, our results may suggest a mechanism by which neutrophils might affect antitumor immunity following other inflammation-inducing cancer therapies. Our findings lay the foundation for the rational design of PDT regimens that lead to optimal enhancement of antitumor immunity in a clinical setting. Immune-enhancing PDT regimens may then be combined with treatments that result in optimal ablation of primary tumors, thus inhibiting growth of primary tumor and controlling disseminated disease.

Introduction

Photodynamic therapy (PDT) destroys tumor tissue through multiple, interacting mechanisms that include direct photodynamic cell kill, microvascular disruption, and inflammation (1). PDT is traditionally used clinically as a local treatment, with little consideration of its potential effects on disseminated disease. Preclinical evidence suggests that PDT enhances systemic anti-tumor immunity although the mechanism of enhancement is unclear (2). Innate immune cell presence and activation is critical to the development of immunity (3), and innate cell infiltration into the treated tumor bed is a hallmark of PDT (1). Our previous data showed that the strong inflammatory response that contributed substantially to local tumor control was dominated by neutrophils (4). In this report, we explore the possibility that neutrophils participate in the generation of antitumor immunity following PDT.

Neutrophils, originally defined as $Gr1^+CD11b^+$ cells but now generally classified as $Gr1^{Hi}CD11b^+F4/80^-$, actively participate in the elicitation and coordination of immune

Requests for reprints: Sandra O. Gollnick, Photodynamic Therapy Center, Roswell Park Cancer Institute, Elm & Carlton Streets, Buffalo, NY 14263. Phone: 716-845-8877; Fax: 716-845-8920; sandra.gollnick@roswellpark.org.

responses to pathogens in the mouse through (*a*) secretion of chemotactic signals that recruit monocytes and immature dendritic cells (5), (*b*) activation of dendritic cells via cell-to-cell contact and secretion of tumor necrosis factor (TNF)-α (6,7), and (*c*) stimulation of monocyte and T-cell differentiation through secretion of IFN-γ (5,8). The role of $Gr1^+CD11b^+$ cells in induction of antitumor immunity is less well defined. Several recent studies have shown the presence of an immunosuppressive cell population in tumor-bearing hosts that is capable of promoting tumor angiogenesis and suppressing T-cell responses and also expresses Gr1 and CD11b molecules (9–12). However, mouse tumors genetically modified to express various cytokines exhibited increased neutrophil infiltration into the tumor bed, which was followed by enhanced T-cell infiltration and subsequent tumor regression (13–15). Furthermore, depletion of neutrophils reduced the number of $CD8^+$ T cells infiltrating the tumor and tumor regression was abrogated.

We recently reported that in murine tumor models, the degree of neutrophilic infiltration can be controlled by the PDT regimen used [i.e., the photosensitizer dose, light dose (fluence), and light dose rate (fluence rate); ref. 4]. In particular, under low fluence rate conditions, high fluence controls tumors through direct cell kill and vascular disruption (~65% cure rate) but generates minimal intratumor inflammatory response; in contrast, low-fluence treatment maintains vascular integrity and induces a pronounced inflammatory response (~20% cure rate). In this report, we have used two PDT regimens differing in their ability to induce neutrophilic infiltrate into the treated tumor bed as experimental models to probe and elucidate the role played by neutrophils in the stimulation of adaptive antitumor immunity following PDT.

Our findings show for the first time that induction of antitumor immunity following PDT is dependent on neutrophil infiltration into the treated tumor bed, and suggest that neutrophils may be directly stimulating T-cell proliferation and/or survival. Consequently, the presence of high levels of neutrophilic infiltrate at the primary treatment site may serve as a potential clinical indicator of the development of systemic immunity, thus adding an important component that might benefit the control of disseminated disease.

Materials and Methods

Animals and tumor system

Pathogen-free BALB/c mice were obtained from the National Cancer Institute; C. 129S2(B6)-$Cmkar2^{tm1Mwm}$ ($CXCR2^{-/-}$) mice were obtained from The Jackson Laboratory. SCID mice were obtained from the Roswell Park Department of Laboratory Animal Resources. Clone 4 mice that bear T cells transgenic for a T-cell receptor that recognizes the $HA_{533-541}$ peptide presented on $H\text{-}2L^d$ (16) were bred in the Roswell Park Department of Laboratory Animal Resources. All mice were female, of BALB/c background, and were housed in microisolator cages in a laminar flow unit under ambient light. Six- to 10-week-old animals were inoculated s.c. on the right shoulder with 10^6 Colo26 (murine colon carcinoma) or Colo26 cells transfected with hemagglutinin (HA) cDNA (Colo26-HA; ref. 17). I.v. challenge with tumor cells was done by injection of exponentially growing Colo26 cells. The RPCI Institutional Animal Care and Use Committee approved all procedures carried out in this study.

Reagents and antibodies

Clinical-grade, pyrogen-free 2-[1-hexylox-yethyl]-2-devinyl pyropheophorbide-a was obtained from the Roswell Park Pharmacy and reconstituted to 0.4 mmol/L in pyrogen-free 5% dextrose in water (D5W; Baxter Corp.). Rat anti-mouse Gr1 was purchased from PharMingen and rat immunoglobulin G isotype control was from Sigma.

In vivo PDT treatment

Tumor-bearing mice were injected in the tail vein with 0.4 μmol/kg of 2-[1-hexyloxyethyl]-2-devinyl pyropheophorbide-a, followed 24 h later by illumination as previously described (4). A spot of 1.1 cm^2 that contained the tumor was illuminated with 665-nm light produced by a dye laser (375; Spectra Physics) pumped by an argon ion laser (2080; Spectra Physics) to a total dose of 48 J/cm^2 given at 7 mW/cm^2 or 128 J/cm^2 given at 14 mW/cm^2. Control mice were treated with photosensitizer alone or, in the case of tumor challenge and tests for immunologic memory, with photosensitizer alone followed by surgical removal of tumors 24 h later.

Adoptive transfer of immune cells

Spleens and tumor draining lymph nodes (TDLN) were harvested; single-cell suspensions were generated by passage through a metallic mesh, RBC were lysed, and cells were plated for at least 2 h in culture plates at 37°C for the depletion of the adherent populations. The nonadherent lymphocytic population was collected, washed, resuspended at 10^7 cell/mL, and injected i.v. (2×10^6 per mouse) 48 h before PDT treatment. SCID mice were reconstituted with 15×10^6 splenocytes. The isolation of $CD8^+$ T cells from TDLN cell suspensions was done by negative selection with MACS columns (Miltenyi Biotec; purity >95%).

Assessment of lung tumor growth

TDLN cells isolated from control or PDT-treated mice (2×10^6 per mouse) were transferred to naïve mice as described above. Recipient mice were injected i.v. with exponentially growing Colo26 cells; 18 days later, the presence of tumors was determined by injection, via an incision in the trachea, of 1 mL of 15% India ink (diluted in PBS). The lungs were removed from the rib cage, weighed, and placed in Fekete's fixative (61% ethanol, 3.2% formaldehyde, 4.1% acetic acid); lung tumors were counted under a dissecting microscope (18).

Flow cytometry

Auxiliary TDLNs or tumors were harvested at the indicated time points and single-cell suspensions were generated (19). Cells were stained with a panel of monoclonal antibodies (mAb) to detect specific cell-surface antigens (CD8, CD11b, CD11c, CD25, CD40, CD44, CD45, CD69, CD80, CD86, Gr1, and F4/80), as previously described (19). The mAbs were directly conjugated with the following fluorochromes: fluorescein (FITC), phycoerythrin, PerCPCy5.5, and allophycocyanin (all from PharMingen, except F4/80, which was purchased from eBioscience). A tetramer of H-$2L^d$ complexed to the HA peptide $HA_{533\text{-}541}$, which is recognized by the clone 4 $CD8^+$ T cells conjugated to phycoerythrin, was provided by the NIH Tetramer Facility, and staining was done as suggested by the provider. For intracellular TNF-α staining, cells were permeabilized with a PBS solution containing 2% bovine serum albumin and 0.5% saponin and incubated with anti-TNF mAb (PharMingen) for 30 min on ice. A BD FACSCalibur was used for flow cytometric analysis; data were acquired from 10,000 (tumor-infiltrating) or 50,000 (TDLN) cells stored in collateral list mode and analyzed using the WinList processing program (Verity Software House, Inc.). At least five mice per group were analyzed. For the determination of the absolute number of specific cell populations, the percentage of each population was multiplied by the number of cells recovered from the respective TDLN.

ELISA for interleukin-6

Tumors were harvested 8 h following treatment and processed as described (19). Protein concentration was determined by the Bio-Rad protein assay (Bio-Rad Laboratories). ELISA

kits specific for interleukin-6 were purchased from R&D Systems and used according to the manufacturer's instructions. At least five mice per group were included.

ELISPOT assay for IFN-γ

BALB/c mice bearing Colo26 tumors were treated with PDT and rested for more than 60 days. Splenocytes from tumor-free mice were examined for tumor responsiveness by ELISPOT assays against irradiated cells pulsed with the tumor-associated antigen AH (the endogenous Colo26 peptide derived from the murine Leukemia virus gp70; ref. 20) or an irrelevant antigen, PA1 (5 μg/mL of each peptide). The number of spot-forming units in each well was enumerated by computer-assisted image analysis using the Zeiss ELISPOT reader system equipped with v 4.1.56 software (Zeiss) by the Roswell Park Cancer Center Immunomonitoring Core facility. The ELISPOT assay was conducted as previously described (21).

In vivo cytotoxicity assay

In vivo cytotoxic assays were done as previously described (22). Briefly, TDLNs were harvested from treated mice 2 days post-PDT and adoptively transferred into naïve BALB/c hosts. Target cells were prepared from naïve mice by labeling a single-cell suspension with PKH26 dye (Sigma) for 4 min at 2 μmol/L according to the manufacturer's instructions. The resulting red population was separated in two equal fractions, one of which was labeled with 0.1 μmol/L carboxyfluorescein diacetate, succinimidyl ester (referred to as CFSE; Molecular Probes) and the other with 1 μmol/L CFSE for 2 min. The lower intensity labeled fraction was pulsed for 1.5 h with an irrelevant peptide PA1 (23); the high intensity labeled fraction was pulsed with the Colo26-specific peptide AH1 (20). Equal cell numbers from both populations were admixed and injected into recipient mice. Twenty-four hours later, peripheral blood was collected, RBC were lysed, and cells were fixed and then run on a FACSCalibur flow cytometer. Specific cytotoxicity was calculated according to the formula [1 – (% AH1 cells/% positive PA1 cells)] × 100%.

$Gr1^+$ cell depletion

Depletion of $Gr1^+$ cells was achieved using anti-Gr1 antibodies (100 μg/mouse i.p.) administered 24 h before treatment and immediately after PDT treatment. Control animals were injected as above with the appropriate isotype. The depletion of the tumor-infiltrating $Gr1^+$ cell population was confirmed by flow cytometry (data not shown).

In vivo T-cell proliferation

Splenocytes were harvested from clone 4 mice, RBC were lysed, and the resulting cell populations were plated for at least 2 h in culture plates at 37°C for the depletion of the adherent populations. The resulting cell populations were washed and resuspended in HBSS at a concentration of 10^7/mL. Cells were stained with CFSE at a concentration of 5 μmol/L for 4 min and then washed once with fetal bovine serum and thrice with complete medium. Cells were counted and 2×10^6 CFSE cells were adoptively transferred into BALB/c mice bearing Colo26-HA tumors. Seven days after PDT treatment, regrowing tumors were harvested, digested with collagenase, and the resulting single-cell suspensions were stained for flow. The percentage of $CFSE^{lo}$ cells was determined between groups by gating on cells that were $CD3^+CD8^+$tet-HA^+ and had diluted their CFSE dye. For cell analysis, at least 500,000 events per animal were collected.

Statistical evaluation

All measured values are presented as mean ± SE. Student's *t* test with Welch's correction was used for comparison between groups in all of the experiments. The term "significant" in the text represents a *P* value of ≤0.05.

Results

Induction of antitumor immunity by PDT is regimen dependent and correlates with induction of acute local inflammation

Figure 1*A* shows the effect of tumor exposure to high-fluence (128 J/cm^2) and low-fluence (48 J/cm^2) PDT on neutrophilic (Gr1^{Hi}CD11b$^+$) infiltrate into the post-PDT tumor bed for Colo26 and Colo26 transfected with the HA antigen (Colo26-HA) tumors. The data are consistent with our earlier work (4) in that low-fluence PDT resulted in significantly higher numbers of infiltrating Gr1^{Hi}CD11b$^+$ cells than high-fluence PDT in both Colo26 and Colo26-HA tumors. Further phenotypic analysis of the infiltrating cell population showed that fewer than 10% of the Gr1^{Hi}CD11b$^+$ cells that infiltrate the tumor bed following low-fluence PDT express the monocyte/macrophage marker F4/80, whereas CD11b$^+$ cells that express low levels of Gr1 are >70% F4/80$^+$; Gr1^{Lo} expressing cells make up <20% of the total Gr1-expressing cells (Fig. 1*B*). These results indicate that neutrophils dominate the tumor infiltrate following PDT.

To test the hypothesis that induction of acute local inflammation by PDT resulted in enhanced antitumor immunity, Colo26 tumor–bearing mice were treated with low-fluence PDT (hereafter referred to as high-inflammation PDT), high-fluence PDT (hereafter referred to as low-inflammation PDT), or photosensitizer alone (control). Auxiliary TDLN were harvested from treated and control mice 2 days after PDT and adoptively transferred into naïve BALB/c mice. Recipient mice were challenged by injection with 10^5 Colo26 cells i.v. to induce lung tumors; 18 days later, lungs were harvested and weighed (Fig. 1*C*). In a nonimmune mouse, tumor cells establish colonies in the lung, which results in increased lung weight. An immune mouse will eliminate most of the tumor cells, resulting in fewer colonies, which will be reflected in a reduced lung weight as compared with a nonimmune mouse. Naïve non–tumor-bearing animals have lungs weighing ~450 mg (data not shown). Lungs harvested from recipient mice receiving TDLN cells isolated from mice 2 days after high-inflammation PDT weighed less than lungs of mice receiving TDLN cells from low-inflammation PDT–treated mice. Both conditions yielded significantly lighter lungs than mice receiving TDLN cells from control mice whose tumors were surgically removed 24 h following photosensitizer injection, thus suggesting that both PDT regimens result in enhanced primary antitumor immune response.

To determine whether the observed antitumor immune response was durable, the ability of splenocytes isolated from mice whose tumors were ablated by PDT or surgically removed to confer tumor protection was evaluated 60 days posttreatment by SCID reconstitution experiments (Fig. 1*D*). SCID mice received 15×10^6 splenocytes from the respective groups and challenged with an i.v. injection of a tumorigenic dose of Colo26 cells. Splenocytes isolated from mice cured with high-inflammation PDT were able to control lung tumor growth significantly better than splenocytes isolated from mice whose tumors were cured by low-inflammation PDT or were surgically removed. Splenocytes isolated from mice whose tumors were cured by low-inflammation PDT did not control lung tumor growth. Thus, it seems that immune cells isolated from low-inflammation PDT are able to mount a primary immune response (Fig. 1*C*) but not a memory immune response (Fig. 1*D*), and that induction of acute local inflammation by high-inflammation PDT leads to establishment of antitumor memory.

Induction of acute local inflammation results in increased numbers of activated tumor-specific CD8$^+$ T cells

PDT-enhanced antitumor immunity has previously been attributed to the presence of tumor-specific CD8$^+$ T cells (24,25); CD8$^+$ T cell–depleted TDLN cells isolated from mice exposed to high-inflammation PDT were unable to transfer antitumor immunity (data not shown). Therefore, we determined whether induction of acute local inflammation was accompanied by changes in the number and/or function of primary immune effector CD8$^+$ T cells. Because the numbers of endogenous tumor-specific T cells were below detectable levels in the parental tumor model (26), we availed ourselves of a mouse strain, clone 4 (16), which bears T cells transgenic for a T-cell receptor that recognizes the ^{HA}533-541 peptide presented on H-2L^d molecules. Naïve transgenic CD8$^+$ T cells were isolated from clone 4 mice and adoptively transferred (2×10^6 cells) into BALB/c mice bearing Colo26-HA tumors. Tumors of the recipient mice were subjected to PDT and TDLN cells were isolated 1 day later. Colo26-HA tumor–bearing mice injected with photosensitizer but not exposed to light were used as controls. Tumor-specific effector T cells were identified as being tet-HA$^+$CD8$^+$CD44^{hi}. Activated tumor-specific effector T cells were defined by the presence of the early activation antigen CD69 (tet-HA$^+$CD8$^+$CD44$^+$CD69$^+$). Figure 2*A* depicts representative flow cytometry panels identifying tumor-specific CD8$^+$ T-cell effectors. The percentage of tumor-specific effector T cells present in the TDLNs was similar among the groups (Fig. 2*B, left*), suggesting that the adoptively transferred clone 4 T cells were recruited to these lymph nodes equally. However, TDLNs recovered from mice treated with high-inflammation PDT were highly enlarged and harbored significantly more cells than TDLNs isolated from either mice treated with low-inflammation PDT or control mice treated with photosensitizer alone (Fig. 2*B, right*). The increase in cell number following treatment with high-inflammation PDT was accompanied by a significant increase in both the frequency (tet-HA$^+$CD8$^+$CD44$^+$CD69$^+$; 40 cells/50,000 for high-inflammation versus ~20 cells/50,000 for the low inflammation and control groups) and the number of activated effector cells present in TDLNs as compared with the other groups (control; Fig. 2*C, left*). The same trend was observed when activated effector tumor-specific CD8$^+$ T cells (tet-HA$^+$CD8$^+$CD44$^+$) were defined by the expression of a second activation marker, CD25; more effector cells expressed CD25 following induction of acute local inflammation (Fig. 2*C, right*). In addition, more TDLN immune cells isolated from mice following induction of acute local inflammation by treatment with high-inflammation PDT secreted IFN-γ in response to cells pulsed with AH1 peptide derived from the endogenous Colo26 tumor antigen gp70 (20) than TDLN cells isolated from mice treated with low-inflammation PDT or control mice (Fig. 2*D*). Furthermore, spleens isolated 60 days after treatment from mice cured with high-inflammation PDT contained significantly more tumor-specific IFN-γ–secreting immune cells ($65.18 \pm 12.35/10^6$ spleen cells) than those from mice either cured with low-inflammation–induced PDT treatment ($16.98 \pm 5.16/10^6$ spleen cells) or had their tumors surgically removed ($27.05 \pm 11.21/10^6$ spleen cells). Thus, it seems that more tumor-specific activated effector T cells were generated following induction of acute local inflammation at the tumor site and that this resulted in a larger pool of tumor-specific immune memory cells.

Neutrophils regulate enhancement of tumor-specific T cells by high-inflammation PDT

Previous studies have shown that neutrophils play a role in establishment of pathogen-specific, T-cell–dependent immune responses (27,28). Consequently, the effect of depletion of neutrophils on T-cell activation and function after PDT was examined by the administration of anti-Gr1 depleting antibodies. Tumor-bearing mice were treated with either anti-Gr1 or isotype antibodies followed by treatment with high-inflammation PDT, and the number of tumor-specific CD8$^+$ effector T cells was determined with flow cytometry 1 day post-PDT. The absolute number of tumor-specific CD8$^+$ effector T cells

was significantly decreased in the absence of $Gr1^+$ cells (Fig. 3*A*). The number of tumor-specific T cells present in the treated tumor 7 days after high-inflammation PDT was also significantly decreased in the absence of $Gr1^+$ cells (Fig. 3*B*). Our previous studies have shown that treatment with anti-Gr1 antibodies significantly reduces tumor response to high-inflammation PDT (4).

The function of TDLN immune cells following induction of acute local inflammation by PDT in mice depleted of $Gr1^+$ cells was determined using *in vivo* cytotoxic assays against the endogenous Colo26 antigen AH1 (Fig. 3*C*). The cytotoxic ability of TDLN cells from mice depleted of $Gr1^+$ cells was significantly reduced in comparison with isotype-treated mice, which is likely a reflection of the reduced number of effector cells present following anti-Gr1 treatment.

Gr1 is expressed on neutrophils, macrophages, plasmacytoid dendritic cells, and memory T cells (29–31); therefore, the results reported above could reflect the effect of depletion of populations other than neutrophils that are involved in T-cell activation. To address these issues, the activation state of tumor-specific T cells following treatment of Colo26-HA tumors with high-inflammation PDT was examined in mice lacking the chemokine receptor CXCR2, which is required for neutrophil migration into tissue. Mice lacking CXCR2 ($CXCR2^{-/-}$) have intact $Gr1^+$ populations (32) and normal monocyte/macrophage, T-cell (32,33), and dendritic cell (34) migration, but impaired neutrophil migration to peripheral sites including the tumor (32,33). The basal level of neutrophils present in Colo26-HA tumors of $CXCR2^{-/-}$ mice was significantly less than in BALB/c mice (Fig. 4*A*) and did not increase significantly after PDT treatment.

Phenotypic analysis of the $CD8^+$ tumor-specific effector T-cell population isolated from TDLNs indicated that this population was significantly reduced in $CXCR2^{-/-}$ mice following treatment with high-inflammation PDT as compared with wild-type mice (Fig. 4*B*). Thus, it seems that neutrophils play a critical role in the enhancement of tumor-specific immunity following tumor treatment with high-inflammation PDT.

Neutrophils gain access to the TDLN following high-inflammation PDT but do not influence dendritic cell maturation

Neutrophils have been shown to capture live bacteria from the skin on intradermal Bacillus Calmette-Guerin (BCG) vaccination and shuttle them to the draining lymph nodes (35). To determine whether neutrophils were present in TDLNs following high-inflammation PDT, TDLN cells were harvested from Colo26 tumor–bearing mice following high-inflammation PDT and analyzed by flow cytometry for the expression of Gr1, CD11b, and F4/80 (Fig. 5*A*). A small proportion of the $Gr1^{Hi}CD11b^+$ population expressed F4/80, whereas cells that expressed lower levels of Gr1 strongly reacted with F4/80 and most likely represented monocyte/macrophage populations. Because activated T cells and some memory T cells also express Gr1, we further analyzed the $Gr1^{Hi}CD11b^+$ population for expression of CD3 and CD8. Approximately 2% of the $Gr1^{Hi}CD11b^+$ cells expressed CD3 and CD8 (data not shown). Thus, it seems that the majority of the $Gr1^{Hi}CD11b^+$ cells in the TDLN were neutrophils and that neutrophils gained access to the TDLN following PDT. Kinetic analysis of neutrophilic infiltration of TDLNs revealed that PDT significantly increased the number of $Gr1^{Hi}CD11b^+F4/80^-$ cells present in the TDLN 8, 24, and 48 h following treatment (Fig. 5*B*).

Neutrophils have been shown to drive dendritic cell maturation by licensing through TNF-α (6), and we have shown that PDT treatment results in increased activation of antigen-presenting cells, including dendritic cells (36). It is possible that neutrophils regulate tumor-specific T cells following PDT indirectly by interacting with dendritic cells. To test this

hypothesis, we first examined the effect of PDT on expression of TNF-α by neutrophils. Intracellular staining for TNF-α revealed that more neutrophils in the TDLN express TNF-α 48 h following high-inflammation PDT (Fig. 5*C*). These results suggest that following high-inflammation PDT, neutrophils have the potential to drive dendritic cell maturation, which could result in increased T-cell activation. Therefore, we examined the phenotype of dendritic cells in the TDLNs of animals treated 48 h prior with high-inflammation PDT in the absence or presence of neutrophils. Dendritic cells were identified by expression of CD11c; mature dendritic cells express increased levels of CD40, CD80, CD86, and MHC class II molecules (IA^d). Depletion of $Gr1^+$ cells had no effect on the number of $CD11c^+CD40^+$ (Fig. 5*D*), $CD11c^+CD80^+$, $CD11c^+CD86^+$, or $CD11c^+IA^{d+}$ dendritic cells (data not shown). These results suggest that neutrophils do not exert their immunomodulating role via licensing of dendritic cells following high-inflammation PDT.

Neutrophils are critical to the expansion of tumor-specific T cells following high-inflammation PDT

The cellularity of the TDLNs was significantly decreased in $CXCR2^{-/-}$ mice (Fig. 6*A*) and in mice depleted of $Gr1^+$ cells following high-inflammation PDT (Fig. 6*B*). To determine if the decrease in cellularity was accompanied by a decrease in T-cell proliferation, clone 4 T cells were labeled with CFSE before their adoptive transfer into Colo26-HA tumor–bearing $Gr1^+$ depleted or isotype control mice. Mice were treated with high-inflammation PDT and the degree of tumor-specific (tet-$HA^+CD3^+CD8^+$) T-cell proliferation in the treated tumor bed was determined 7 days after PDT. The decrease in cellularity in the absence of neutrophils corresponded to a significant decrease in T-cell proliferation following high-inflammation PDT of mice depleted of $Gr1^+$ cells (Fig. 6*C*). These results suggest that neutrophils contribute to either effector T-cell proliferation or survival.

Discussion

In this study, we have examined the effect of neutrophils on enhancement of antitumor immunity by PDT. We used two PDT regimens that differ in their ability to induce neutrophilic infiltration into the treated tumor bed and reported that neutrophil migration into the tumor bed enhanced the magnitude of the tumor-specific primary immune response as well as the establishment of memory antitumor immune responses. Neutrophils regulated the number of tumor-specific $CD8^+$ T cells in the TDLN and affected the number of tumor-specific $CD8^+$ T cells and the degree of T-cell proliferation at the tumor site, but seemed to have no effect on dendritic cell maturation or T-cell migration. This suggests that neutrophils directly influence T-cell proliferation and/or survival following PDT. To our knowledge, this is the first report to identify tumor-infiltrating neutrophils as being critical to the enhancement of tumor-specific T cells and the generation of antitumor immunity following PDT. In addition, our data suggest that neutrophils can contribute to the induction of antitumor immunity by other modalities through direct interaction with tumor-specific $CD8^+$ T cells.

Our study used the anti-Gr1 RB6-8C5 antibody to deplete neutrophils, which is a well-established procedure (15,27,37). However, Gr1 is also expressed on plasmacytoid dendritic cells and macrophages (29,30), which are well-characterized stimulators of T cells. However, depletion with anti-Gr1 antibody did not affect the number of CD11c cells present in TDLNs following PDT (Fig. 5*D*), whereas use of $CXCR2^{-/-}$ mice, which exhibit impaired neutrophil migration but normal monocyte/macrophage and dendritic cell migration (33,34), produced similar results to those observed following depletion of $Gr1^+$ cells, supporting our conclusion that neutrophils play a critical role in enhancement of $CD8^+$ T-cell activation by PDT.

Neutrophil-$CD8^+$ T-cell cross talk has previously been correlated with the induction of antitumor and pathogen specific immunity (15,27,28,38,39). A predominant mechanism involves neutrophil-dendritic cell interaction, with an important role assigned to TNF-α expressed on neutrophils, which can increase dendritic cell activation. Because the phenotypic maturation of dendritic cells following PDT is not affected by the administration of anti-Gr1 antibodies (Fig. 5), then neutrophils seem to affect $CD8^+$ T cell–mediated antitumor immunity following PDT by other means. However, it is possible that neutrophil depletion affects dendritic cell function, which was not examined in the current study.

Neutrophils have also been shown to indirectly affect T-cell trafficking through the accessory function of activated monocytes (39) and through expression of chemotactic factors that regulate T-cell migration (5,40). Depletion of $Gr1^+$ cells before high-inflammation PDT reduced the frequency of tumor-specific T cells present in TDLNs, implicating these cells in regulation of T-cell migration. However, memory T cells express Gr1 (31), and it is possible that the reduction in frequency is due to direct elimination of this subset of T cells. $CXCR2^{-/-}$ mice do not have impaired T-cell migration (41,42) and the frequency of tumor-specific $CD8^+$ T cells was similar in wild-type and $CXCR2^{-/-}$ mice following high-inflammation PDT, suggesting that neutrophils are not affecting T-cell migration following PDT. Little is known about the effect of PDT on T-cell trafficking, and more direct analysis of this and the effect of neutrophils on T-cell trafficking following PDT is needed before a role for neutrophils in regulating T-cell trafficking can be determined.

Our study indicates a direct role for neutrophils in T-cell proliferation because fewer proliferating tumor-specific T cells were present in the tumor bed following PDT in the absence of neutrophils (Fig. 6). Neutrophils have been shown to sustain pathogenic $CD8^+$ T cells in the heart (43) and to affect T-cell activation and proliferation in inflammatory setting through expression of MHC class II molecules (44,45). PDT also stimulates MHC class II molecule expression by neutrophils (46), suggesting that neutrophils have the potential to directly affect T-cell proliferation following PDT. This possibility is supported by the presence of neutrophils in the TDLN following PDT because this is the major site of tumor-specific T-cell activation and proliferation.

Neutrophils lack expression of CC chemokine receptor 7 and do not seem to have access into lymph nodes; however, a recent report from Abadie et al. (35) showed that neutrophils migrate into draining lymph nodes via the lymphatics following *Mycobacterium bovis* BCG vaccination. Thus, it is possible that PDT-induced inflammation enables neutrophils to access TDLNs. It is also possible that given the small size of the animal model, PDT of mice results in photodamage of the nearby TDLNs, which allows unregulated cell migration into these nodes. However, the dose of PDT used to induce high inflammation is relatively low and we have not observed damage to TDLNs following this treatment regimen.

Cancer survival rates decrease in the presence of metastases,[1] and there is increased interest in generation of therapies capable of enhancing antitumor immunity. We have recently shown that local PDT of primary murine tumors can control the growth of tumors outside the treatment field (25). Furthermore, data from our laboratory indicate that aminolevulinic acid PDT of basal cell carcinoma enhanced tumor-specific immune responses in patients.[2] It is well established that clinical PDT results in inflammatory responses (1), but the degree of neutrophilic infiltration is unknown (47,48). The results presented here indicate that an examination of the local tissue response following clinical PDT is warranted.

[1]Ries LAG, Eisner MP, Kosary CL, et al. SEER cancer statistics review, 1975-2003. Bethesda (MD): National Cancer Institute; 2006. Available from: http://seer.cancer.gov/csr/1975_2003/.
[2]S.O. Gollnick, in preparation.

It should be noted that the high-inflammation PDT regimen used in the current study resulted in minimal tumor growth control at the primary treatment site; low-inflammation PDT was highly effective at controlling primary tumor growth but did not result in durable immune responses. Our findings suggest that combination PDT regimens composed of treatments resulting in optimal induction of antitumor immunity followed by treatments leading to ablation of the primary tumor should be considered. PDT regimens that induce antitumor immunity could also be used in an adjuvant setting with other local treatments, such as surgery, which is effective at controlling primary tumors but has no effect on disseminated disease. Thus, PDT regimens capable of inducing antitumor immunity can be rationally designed, which has the potential to expand the use of this treatment modality.

Acknowledgments

Grant support: NIH grants CA55791 and CA98156 and in part by Roswell Park Cancer Center Support Grant CA16056.

We thank Dr. Sara L. Schneider of the Roswell Park Cancer Center Immunomonitoring Core for providing valuable assistance in the design and interpretation of the ELISPOT analyses, and Drs. David Bellnier (Department of Cellular Stress Biology, Roswell Park Cancer Institute) and James Clements (Department of Immunology, Roswell Park Cancer Institute) for their critical comments on the manuscript.

References

1. Dougherty TJ, Gomer CJ, Henderson BW, et al. Photodynamic therapy. J Natl Cancer Inst 1998;90:889–905. [PubMed: 9637138]
2. Castano AP, Mroz P, Hamblin MR. Photodynamic therapy and anti-tumour immunity. Nat Rev Cancer 2006;6:535–45. [PubMed: 16794636]
3. Lee HK, Iwasaki A. Innate control of adaptive immunity: dendritic cells and beyond. Semin Immunol 2007;19:48–55. [PubMed: 17276695]
4. Henderson BW, Gollnick SO, Snyder JW, et al. Choice of oxygen-conserving treatment regimen determines the inflammatory response and outcome of photodynamic therapy of tumors. Cancer Res 2004;64:2120–6. [PubMed: 15026352]
5. Nathan C. Neutrophils and immunity: challenges and opportunities. Nat Rev Immunol 2006;6:173–82. [PubMed: 16498448]
6. van Gisbergen KP, Geijtenbeek TB, van Kooyk Y. Close encounters of neutrophils and DCs. Trends Immunol 2005;26:626–31. [PubMed: 16182604]
7. Bennouna S, Denkers EY. Microbial antigen triggers rapid mobilization of TNF-αto the surface of mouse neutrophils transforming them into inducers of high-level dendritic cell TNF-αproduction. J Immunol 2005;174:4845–51. [PubMed: 15814711]
8. Ethuin F, Gerard B, Benna JE, et al. Human neutrophils produce interferon gamma upon stimulation by inter-leukin-12. Lab Invest 2004;84:1363–71. [PubMed: 15220936]
9. Almand B, Clark JI, Nikitina E, et al. Increased production of immature myeloid cells in cancer patients: a mechanism of immunosuppression in cancer. J Immunol 2001;166:678–89. [PubMed: 11123353]
10. Gabrilovich DI, Velders MP, Sotomayor EM, Kast WM. Mechanism of immune dysfunction in cancer mediated by immature Gr-1^{+} myeloid cells. J Immunol 2001;166:5398–406. [PubMed: 11313376]
11. Gabrilovich DI, Bronte V, Chen SH, et al. The terminology issue for myeloid-derived suppressor cells. Cancer Res 2007;67:425. [PubMed: 17210725]
12. Serafini P, De SC, Marigo I, et al. Derangement of immune responses by myeloid suppressor cells. Cancer Immunol Immunother 2004;53:64–72. [PubMed: 14593498]
13. Cavallo F, Giovarelli M, Gulino A, et al. Role of neutrophils and $CD4^{+}$ T lymphocytes in the primary and memory response to nonimmunogenic murine mammary adenocarcinoma made immunogenic by IL-2 gene. J Immunol 1992;149:3627–35. [PubMed: 1358974]

14. Graf MR, Prins RM, Merchant RE. IL-6 secretion by a rat T9 glioma clone induces a neutrophil-dependent antitumor response with resultant cellular, antiglioma immunity. J Immunol 2001;166:121–9. [PubMed: 11123284]
15. Stoppacciaro A, Melani C, Parenza M, et al. Regression of an established tumor genetically modified to release granulocyte colony-stimulating factor requires granulocyte-T-cell cooperation and T cell-produced interferon γ. J Exp Med 1993;178:151–61. [PubMed: 7686211]
16. Morgan DJ, Liblau R, Scott B, et al. CD8(+) T cell-mediated spontaneous diabetes in neonatal mice. J Immunol 1996;157:978–83. [PubMed: 8757600]
17. Lu Z, Yuan L, Zhou X, et al. CD40-independent pathways of T-cell help for priming of CD8(+) cytotoxic T lymphocytes. J Exp Med 2000;191:541–50. [PubMed: 10662799]
18. Cerosaletti KM, Blieden TM, Harwell LW, et al. Alteration of the metastatic potential of Line 1 lung carcinoma cells: opposite effects of class I antigen induction by interferons versus DMSO of gene transfection. Cell Immunol 1990;127:299–310. [PubMed: 1691690]
19. Gollnick SO, Liu X, Owczarczak B, Musser DA, Henderson BW. Altered expression of interleukin 6 and interleukin 10 as a result of photodynamic therapy *in vivo*. Cancer Res 1997;57:3904–9. [PubMed: 9307269]
20. Huang AYC, Gulden PH, Woods AS, et al. The immunodominant major histocompatibility complex class I-restricted antigen of a murine colon tumor derives from an endogenous retroviral gene product. Proc Natl Acad Sci U S A 1996;93:9730–5. [PubMed: 8790399]
21. Gollnick SO, Vaughan LA, Henderson BW. Generation of effective anti-tumor vaccines using photodynamic therapy. Cancer Res 2002;62:1604–8. [PubMed: 11912128]
22. Barber DL, Wherry EJ, Ahmed R. Cutting edge: rapid *in vivo* killing by memory CD8 T cells. J Immunol 2003;171:27–31. [PubMed: 12816979]
23. Lethe B, Van den Eynde B, Van Pel A, Corradin G, Boon T. Mouse tumor rejection antigens P815A and P815B: two epitopes carried by a single peptide. Eur J Immunol 1992;22:2283. [PubMed: 1381312]
24. Korbelik M, Krosl G, Krosl J, Dougherty GJ. The role of host lymphoid populations in the response of mouse EMT6 tumor to photodynamic therapy. Cancer Res 1996;56:5647–52. [PubMed: 8971170]
25. Kabingu E, Vaughan L, Owczarczak B, Ramsey KD, Gollnick SO. $CD8^+$ T cell-mediated control of distant tumours following local photodynamic therapy is independent of $CD4^+$ T cells and dependent on natural killer cells. Br J Cancer 2007;96:1839–48. [PubMed: 17505510]
26. Marzo AL, Lake RA, Robinson BWS, Scott B. T-cell receptor transgenic analysis of tumor-specific CD8 and CD4 responses in the eradication of solid tumors. Cancer Res 1999;59:1071–9. [PubMed: 10070965]
27. Ismail HF, Fick P, Zhang J, Lynch RG, Berg DJ. Depletion of neutrophils in IL-10(−/−) mice delays clearance of gastric *Helicobacter* infection and decreases the Th1 immune response to *Helicobacter*. J Immunol 2003;170:3782–9. [PubMed: 12646644]
28. Tateda K, Moore TA, Deng JC, et al. Early recruitment of neutrophils determines subsequent T1/T2 host responses in a murine model of *Legionella pneumophila* pneumonia. J Immunol 2001;166:3355–61. [PubMed: 11207291]
29. Fleming TJ, Fleming ML, Malek TR. Selective expression of Ly-6G on myeloid lineage cells in mouse bone marrow. RB6-8C5 mAb to granulocyte-differentiation antigen (Gr-1) detects members of the Ly-6 family. J Immunol 1993;151:2399–408. [PubMed: 8360469]
30. Nakano H, Yanagita M, Gunn MD. CD11c(+) B220(+)Gr-1(+) cells in mouse lymph nodes and spleen display characteristics of plasmacytoid dendritic cells. J Exp Med 2001;194:1171–8. [PubMed: 11602645]
31. Walunas TL, Bruce DS, Dustin L, Loh DY, Bluestone JA. Ly-6C is a marker of memory $CD8^+$ T cells. J Immunol 1995;155:1873–83. [PubMed: 7543536]
32. Cacalano G, Lee J, Kikly K, et al. Neutrophil and B cell expansion in mice that lack the murine IL-8 receptor homolog. Science 1994;265:682–4. [PubMed: 8036519]
33. Shimizu M, Yoshimoto T, Sato M, et al. Roles of CXC chemokines and macrophages in the recruitment of inflammatory cells and tumor rejection induced by Fas/Apo-1 (CD95) ligand-expressing tumor. Int J Cancer 2005;114:926–35. [PubMed: 15645421]

34. Yoneyama H, Matsuno K, Matsushimaa K. Migration of dendritic cells. Int J Hematol 2005;81:204–7. [PubMed: 15814331]
35. Abadie V, Badell E, Douillard P, et al. Neutrophils rapidly migrate via lymphatics after *Mycobacterium bovis* BCG intradermal vaccination and shuttle live bacilli to the draining lymph nodes. Blood 2005;106:1843–50. [PubMed: 15886329]
36. Gollnick SO, Owczarczak B, Maier P. Photodynamic therapy and anti-tumor immunity. Lasers Surg Med 2006;38:509–15. [PubMed: 16788921]
37. Bennouna S, Bliss SK, Curiel TJ, Denkers EY. Crosstalk in the innate immune system: neutrophils instruct recruitment and activation of dendritic cells during microbial infection. J Immunol 2003;171:6052–8. [PubMed: 14634118]
38. Giovarelli M, Cappello P, Forni G, et al. Tumor rejection and immune memory elicited by locally released LEC chemokine are associated with an impressive recruitment of APCs, lymphocytes, and granulocytes. J Immunol 2000;164:3200–6. [PubMed: 10706711]
39. Suttmann H, Riemensberger J, Bentien G, et al. Neutrophil granulocytes are required for effective bacillus calmette-guerin immunotherapy of bladder cancer and orchestrate local immune responses. Cancer Res 2006;66:8250–7. [PubMed: 16912205]
40. Chertov O, Yang D, Howard OM, Oppenheim JJ. Leukocyte granule proteins mobilize innate host defenses and adaptive immune responses. Immunol Rev 2000;177:68–78. [PubMed: 11138786]
41. Rot A. Endothelial cell binding of NAP-1/IL-8: role in neutrophil emigration. Immunol Today 1992;13:291–4. [PubMed: 1510812]
42. Larsen CG, Anderson AO, Appella E, Oppenheim JJ, Matsushima K. The neutrophil-activating protein (NAP-1) is also chemotactic for T lymphocytes. Science 1989;243:1464–6. [PubMed: 2648569]
43. Grabie N, Hsieh DT, Buono C, et al. Neutrophils sustain pathogenic $CD8^+$ T-cell responses in the heart. Am J Pathol 2003;163:2413–20. [PubMed: 14633613]
44. Fanger NA, Liu C, Guyre PM, et al. Activation of human T cells by major histocompatability complex class II expressing neutrophils: proliferation in the presence of superantigen, but not tetanus toxoid. Blood 1997;89:4128–35. [PubMed: 9166855]
45. Cross A, Bucknall RC, Cassatella MA, Edwards SW, Moots RJ. Synovial fluid neutrophils transcribe and express class II major histocompatibility complex molecules in rheumatoid arthritis. Arthritis Rheum 2003;48:2796–806. [PubMed: 14558085]
46. Sun J, Cecic I, Parkins CS, Korbelik M. Neutrophils as inflammatory and immune effectors in photodynamic therapy-treated mouse SCCVII tumours. Photochem Photobiol Sci 2002;1:690–5. [PubMed: 12665307]
47. Yom SS, Busch TM, Friedberg JS, et al. Elevated serum cytokine levels in mesothelioma patients who have undergone pleurectomy or extrapleural pneumonectomy and adjuvant intra-operative photodynamic therapy. Photochem Photobiol 2003;78:75–81. [PubMed: 12929752]
48. Nseyo UO, Whalen RK, Duncan MR, Berman B, Lundahl SL. Urinary cytokines following photodynamic therapy for bladder cancer. Urology 1990;36:167–71. [PubMed: 2117309]

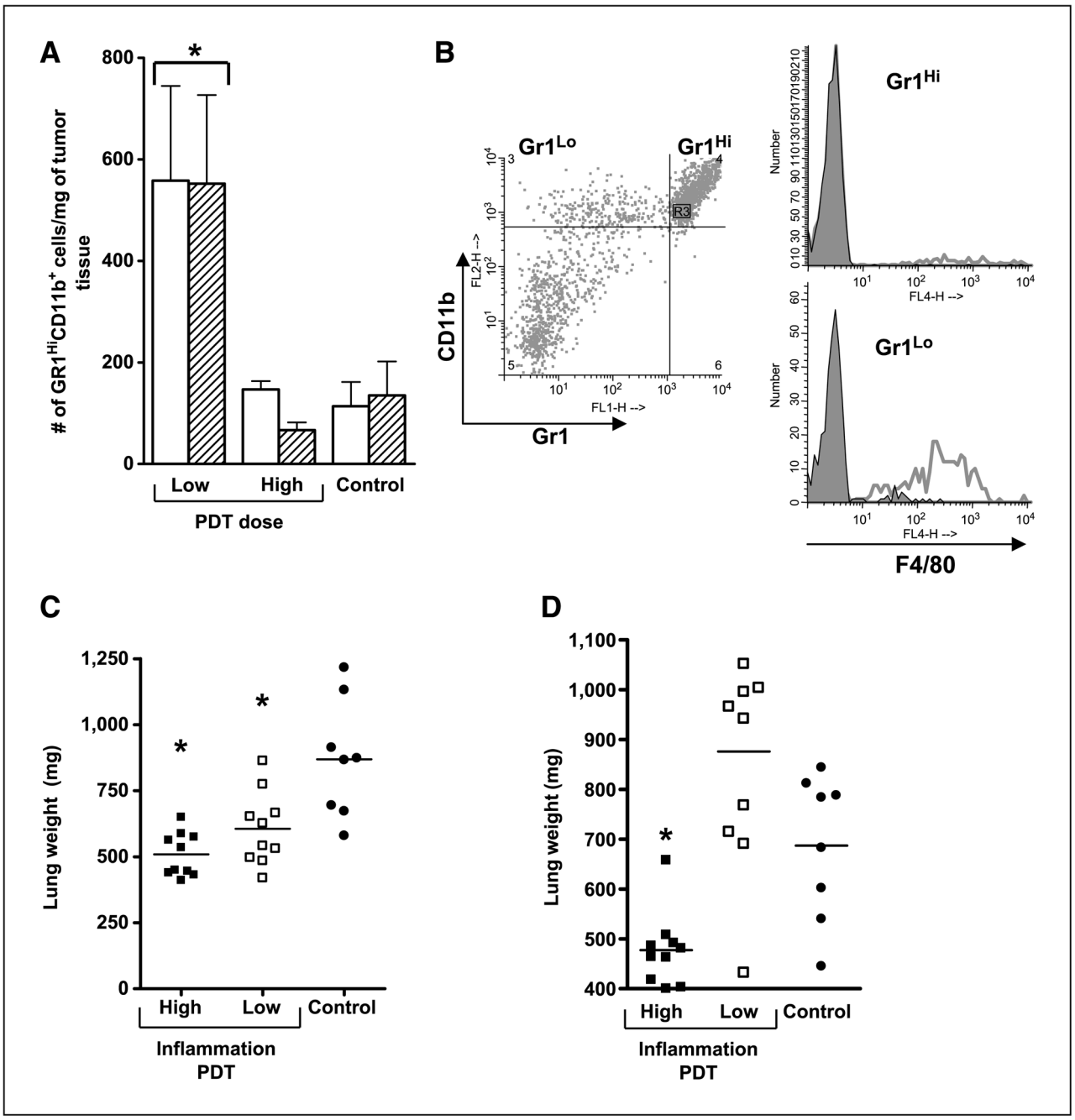

Figure 1.

PDT induces acute local inflammation. *A*, BALB/c mice bearing Colo26 (*open columns*) or Colo26-HA (*hatched columns*) tumors were subjected to low-fluence (48 J/cm^2) or high-fluence (128 J/cm^2) PDT. Tumors were harvested 8 h post-PDT and single-cell suspensions were generated and analyzed by flow cytometry for the presence of Gr1^{Hi}CD11b$^+$ cells as described in Materials and Methods. Results are expressed as the number of Gr1^{Hi}CD11b$^+$ cells per milligram of tumor tissue. Five mice per group were included and the experiment was repeated twice. One representative experiment is shown; *bars*, SE. *, $P < 0.04$, compared with high-fluence PDT. *B*, BALB/c mice bearing Colo26 tumors were subjected to low-dose PDT; tumors were isolated 8 h later and single-cell suspensions were generated

and examined by flow cytometry for expression of CD45, Gr1, CD11b, and F4/80. Representative histograms are shown in which $CD45^+CD11b^+$ cells were gated for either high or low expression of Gr1 (*left*) and examined for expression of F4/80 (*right*). Open histograms in the single color histograms show F4/80 reactivity; closed histograms represent staining with an isotype matched control. *C*, BALB/c mice bearing Colo26 tumors were subjected to high or low local inflammation PDT treatment; control mice were injected with photosensitizer and, 18 h later, instead of light treatment, tumors were removed surgically. TDLNs were harvested 2 d posttreatment and adoptively transferred into naïve BALB/c mice. Recipient mice were challenged with 10^5 Colo26 cells i.v.; 18 d later, lungs were harvested and weighed. *D*, SCID mice were reconstituted with 15×10^6 adherent depleted splenocytes isolated from cured mice 60 d after treatment. Recipient mice were challenged and lungs were harvested and weighed as in *C*. *Symbols*, individual animals; *solid line*, mean. *, $P < 0.02$, compared with control.

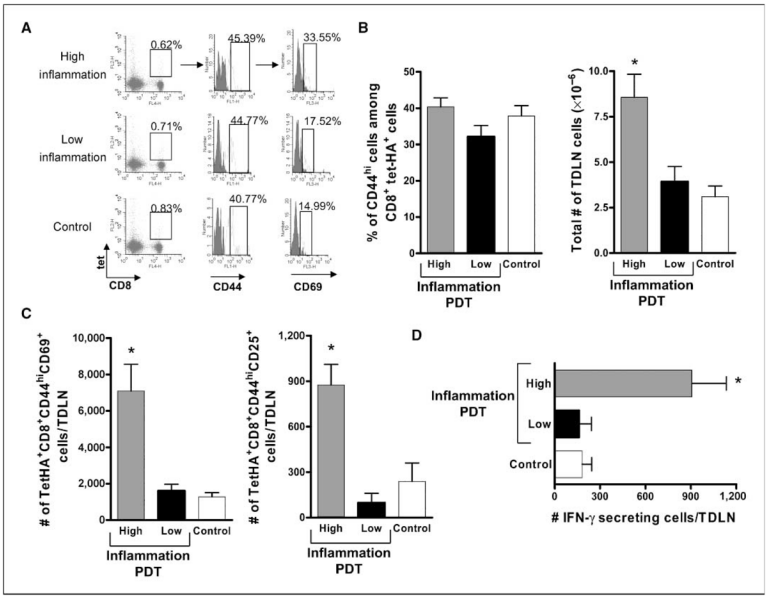

Figure 2.

Enhanced numbers of activated tumor-specific $CD8^+$ T cells in TDLNs of mice following induction of acute local inflammation. BALB/c mice bearing Colo26-HA (*A–C*) or Colo26 (*D*) tumors were subjected to PDT treatments, causing different levels of acute inflammation, or injected with the photosensitizer and not exposed to laser treatment (*Control*). Twenty-four hours later, TDLN were harvested, single-cell suspensions generated, and the phenotype of $CD8^+$ T cells specific for the HA antigen (tet^+) was determined. *A,* flow cytometry depicting staining for tet-HA, CD8, CD44, and CD69. The boxed area in the first column identifies the tet-HA^+CD8^+ T cells. The second column depicts CD44 staining and is gated on the tet-HA^+CD8^+ T-cell population. The third column is gated on the tet-$HA^+CD8^+CD44^{hi}$ population and shows staining for CD69. The numbers indicate percentages of cells in the respective gates. Data from one representative experiment is shown. *B, left,* average percentage of $CD44^{hi}$ cells among the tet-HA^+CD8^+ population from three individual experiments. *Right,* the corresponding average number of live cells, as determined with trypan blue, recovered from the TDLNs. *C,* absolute number of tumor-specific $CD8^+$ T-cell effector cells that expressed CD69 (*left*) and CD25 (*right*) following treatment. Experiments depicted in *B* and *C* were repeated twice with five mice per group; *bars,* SE. *, $P < 0.03$, compared with low-inflammation PDT. *D,* TDLNs were harvested at 24 h posttreatment and single-cell suspensions were generated. The number of cells able to specifically recognize tumor antigen AH1 and secrete IFN-γ as a consequence was determined with ELISPOT assays. Nonspecific staining with an irrelevant peptide (PA1) was subtracted from each group. *Columns,* average number of IFN-γ^+ cells (each group contains at least six mice per group); *bars,* SE. *, $P < 0.01$, compared with low-inflammation PDT.

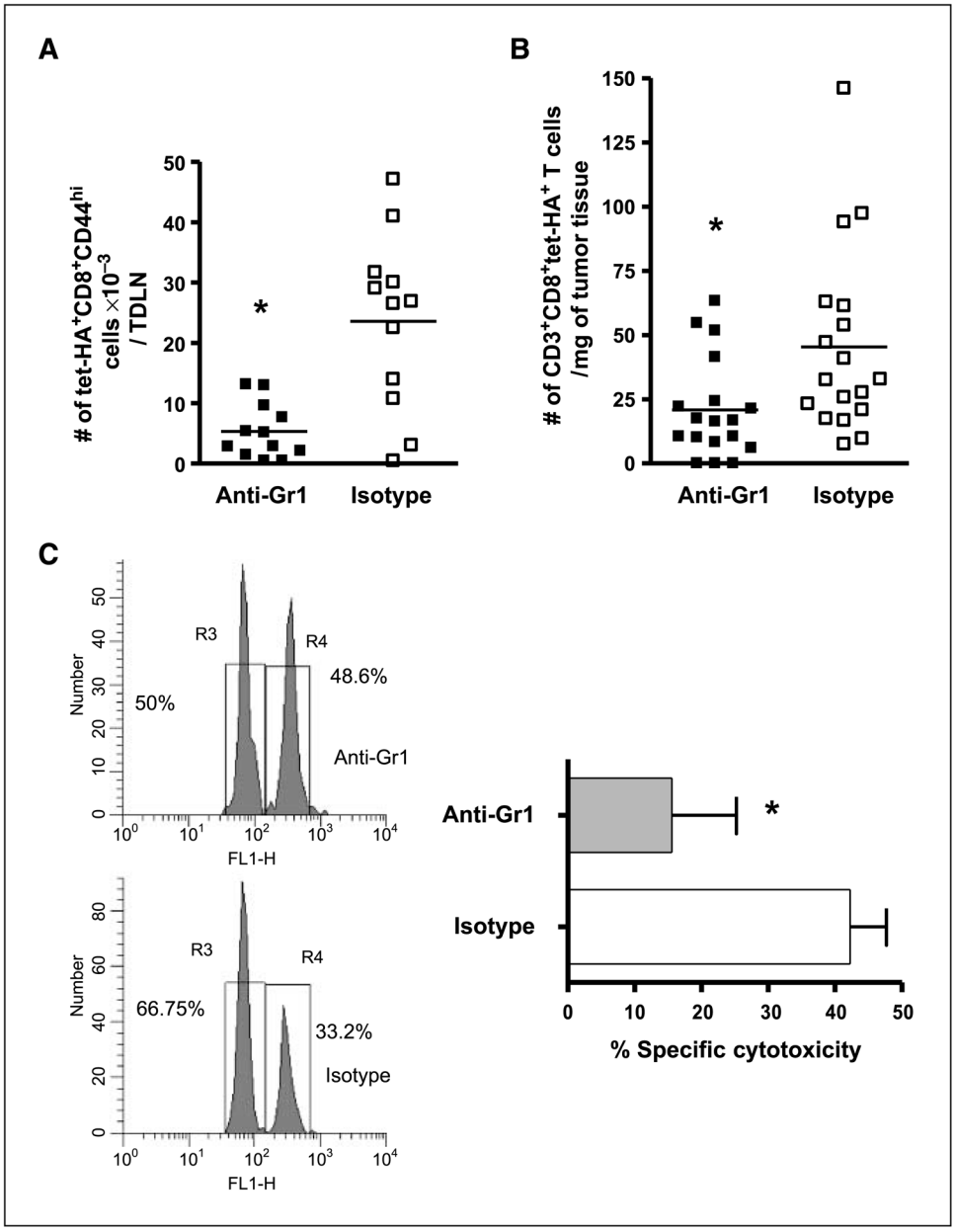

Figure 3.

$Gr1^+$ cells coordinate the adaptive immune response to tumors following induction of acute local inflammation. BALB/c mice bearing Colo26-HA tumors were either depleted of $Gr1^+$ cells with the administration of a Gr1 depleting antibody or injected with an isotype control antibody. Then they were subjected to high-inflammation PDT; TDLNs were harvested after 24 h (*A*) or tumor tissue was collected 7 d later (*B*). The absolute numbers of tumor-specific effectors were determined with flow cytometry, as previously described. *Symbols*, individual animals; *solid line*, mean. *, $P < 0.02$, compared with isotype-treated mice. *C*, BALB/c mice bearing Colo26 tumors were given anti-Gr1 depleting or isotype control antibody and then subjected to high-inflammation PDT. Two days posttreatment, TDLNs were harvested and adoptively transferred into naïve BALB/c mice. *In vivo* cytotoxic assays against the endogenous AH1 antigen or an irrelevant antigen PA1 were done in the recipient mice (n =

5). *Left*, representative histogram. *Right*, cumulative results of two independent experiments each containing five mice, presented as percent specific cytotoxicity. *, $P < 0.03$, compared with isotype-treated mice.

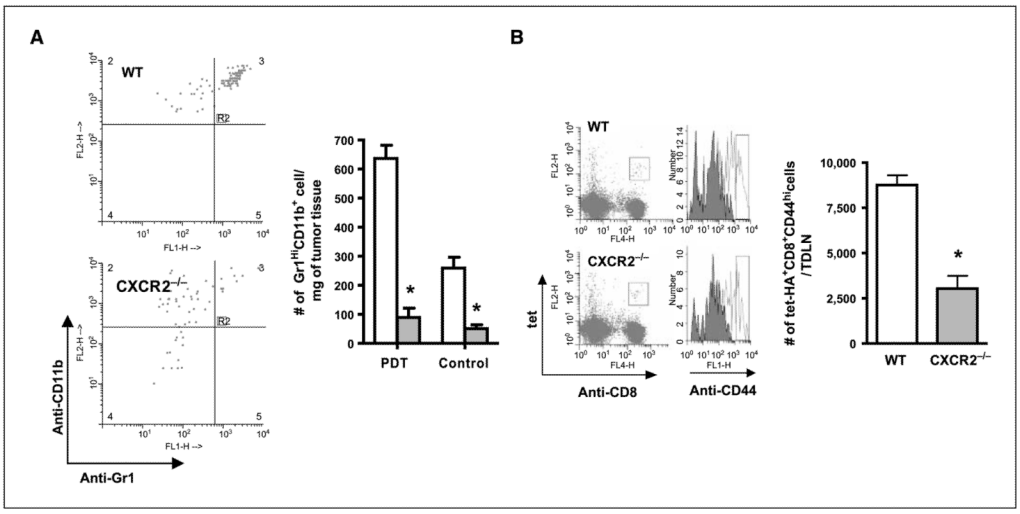

Figure 4.

Neutrophils are critical for activation of $CD8^+$ effector T cells following induction of acute local inflammation. *A*, tumors were harvested 8 h post-PDT or 24 h after injection of photosensitizer (*Control*) from wild-type and $CXCR2^{-/-}$ mice; single-cell suspensions were generated and analyzed by flow cytometry for the presence of $Gr1^{Hi}CD11b^+$ cells as described in Materials and Methods. *Left*, dot plots of the results of staining cells gated for CD45 expression with Gr1 and CD11b specific antibodies from one representative experiment. *Right*, average absolute number of cells ($n = 3$); *open columns*, wild-type mice; *shaded columns*, $CXCR2^{-/-}$ mice. *, $P < 0.04$, compared with wild-type mice. *B*, $CXCR2^{-/-}$ or wild-type (*WT*) mice bearing Colo26-HA tumors were treated with PDT to induce acute local inflammation and the number of tumor-specific $CD8^+$ T effectors was determined as previously described. *Left*, representative histograms; *right*, cumulative data ($n = 10$). *, $P < 0.003$, compared with wild-type mice.

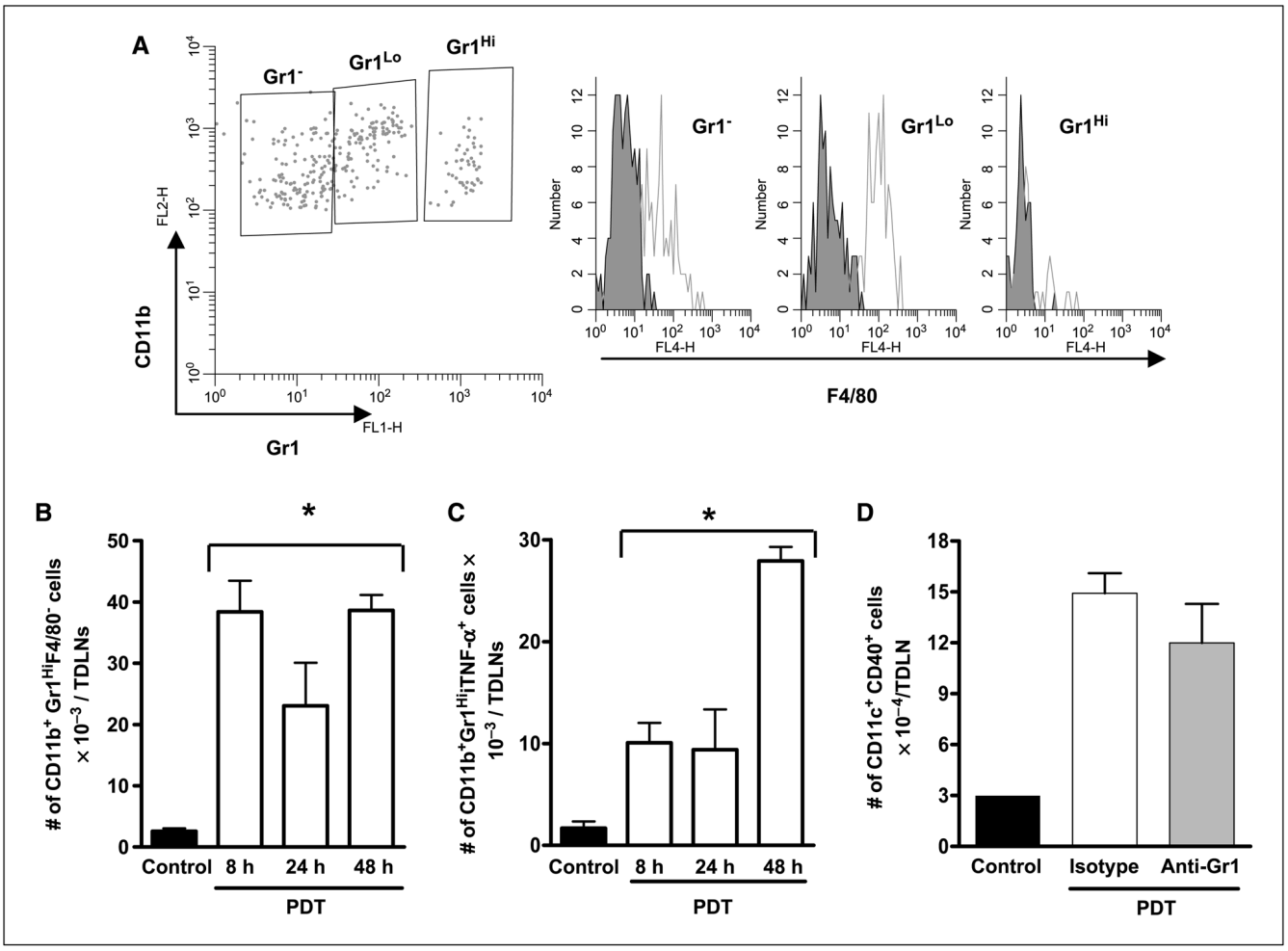

Figure 5.

Effect of neutrophil depletion on dendritic cell phenotype following PDT treatment. TDLNs from tumor-bearing photosensitizer only–treated (*Control*) or high-inflammation PDT–treated mice were harvested at various times posttreatment. Single-cell suspensions were generated and subjected to flow cytometric analysis. *A*, histograms from a representative experiment showing F4/80 expression in $Gr1^{Hi}$ expressing neutrophils. *B* and *C*, *columns*, average number of $CD11b^{+}Gr1^{Hi}F4/80^{-}$ cells (*B*) or $CD11b^{+}Gr1^{Hi}iTNF^{+}$ cells (*C*) per TDLN; *bars*, SE. Experiments were repeated twice with five mice per group. *D*, TDLNs from tumor-bearing high-inflammation PDT–treated mice that were depleted of neutrophils by injection with anti-Gr1 antibody or not (isotype injected) were harvested 48 h posttreatment and single-cell suspensions were generated. Dendritic cells were identified as $CD11c^{+}$ cells and further stained for CD40 expression. *Columns*, average absolute number of $CD11c^{+}CD40^{+}$ cells per TDLN; *bars*, SE. Experiments were repeated twice with five mice per group. *, $P < 0.02$, compared with control.

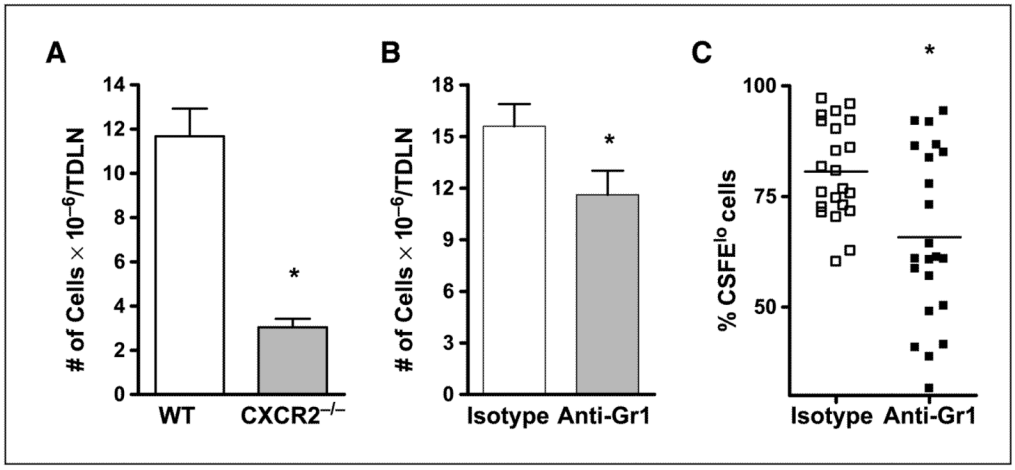

Figure 6.

Neutrophil depletion affects the proliferative ability of tumor-specific T cells following PDT treatment. *A*, CXCR2$^{-/-}$ or BALB/c mice bearing Colo26-HA tumors were subjected to high-inflammation PDT and, 24 h later, TDLNs were harvested, single-cell suspensions were generated, and the number of live cells was determined. *Columns*, average number of cells present; *bars*, SE. Each experiment was repeated twice and contained a minimum of five mice per group. *, $P < 0.002$, compared with wild-type mice. *B*, BALB/c mice bearing Colo26-HA tumors were injected with anti-Gr1 or isotype control antibodies before high-inflammation PDT. Twenty-four hours following PDT, TDLNs were harvested, single-cell suspensions were generated, and the number of live cells was determined. *Columns*, average number of cells present; *bars*, SE. Each experiment was repeated twice and contained a minimum of five mice per group. *, $P < 0.05$, compared with isotype control. *C*, BALB/c mice bearing Colo26-HA were injected with anti-Gr1 or isotype control antibodies before PDT treatment. All mice also received CFSE-labeled clone 4 splenocytes. Tumors were harvested 7 d after PDT treatment, single-cell suspensions were generated, and the percentage of CD3$^+$CD8$^+$tet-HA$^+$ cells that were CFSE^{lo} was determined. Pooled data from 20 mice are shown. *, $P < 0.004$, compared with isotype-treated mice.